June 1986

Cooling by Immersion in Liquid Nitrogen

vita tensor. If we define a three-form B such that $C = *B$, then Eq. (13) can be written as

$$F = dA + \delta B + F^{(0)}, \tag{17}$$

where the codifferential[21] δ of B is defined as $\delta B = -*d*B$ and the two-form $F^{(0)}$ is a solution to the wave equation. Equation (17) is a special case of the Hodge decomposition theorem.[22–24] The Hodge decomposition theorem is the natural generalization of Helmholtz's theorem to an arbitrary dimensional space.

[1]B. P. Miller, Am. J. Phys. **52**, 948 (1984).
[2]D. H. Kobe, Am. J. Phys. **52**, 354 (1984).
[3]N. Schleifer, Am. J. Phys. **51**, 1139 (1983).
[4]A. Shadowitz, *The Electromagnetic Field* (McGraw-Hill, New York, 1975), p. 412.
[5]H. Flanders, *Differential Forms* (Academic, New York, 1963), p. 138.
[6]W. G. V. Rosser, Am. J. Phys. **43**, 502 (1975); **44**, 1221 (1976).
[7]G. Arfken, *Mathematical Methods for Physicists* (Academic, New York, 1970), 2nd ed., pp. 66–70.
[8]W. K. H. Panofsky and M. Phillips, *Classical Electricity and Magnetism* (Addison-Wesley, Reading, MA, 1962), pp. 2–6; Ref. 4, pp. 187–190.
[9]J. R. Reitz, F. J. Milford, and R. W. Christy, *Foundations of Electromagnetic Theory* (Addison-Wesley, Reading, MA, 1979), 3rd ed., p. 19.
[10]N. Tralli, *Classical Electromagnetic Theory* (McGraw-Hill, New York, 1963), pp. 13 and 14. The procedure we use is the same as Tralli, but he assumes Eq. (3) and also assumes that $\nabla \cdot \mathbf{W} = 0$. We prove both.
[11]J. D. Jackson, *Classical Electrodynamics* (Wiley, New York, 1975), 2nd ed., pp. 43–45.
[12]W. Hauser, Am. J. Phys. **38**, 80 (1970).
[13]W. Hauser, *Introduction to the Principles of Electromagnetism* (Addison-Wesley, Reading, MA, 1971), pp. 576–579.
[14]N. Cabibbo and E. Ferrari, Nuovo Cimento **23**, 1147 (1962).
[15]The term $F^{(0)}_{\mu\nu}$ is unnecessary if the boundary conditions are satisfied by the first two terms on the right-hand side of Eq. (11).
[16]Reference 3, p. 1144.
[17]P. A. M. Dirac, Proc. R. Soc. London Ser. A **133**, 60 (1931); Phys. Rev. **74**, 817 (1948).
[18]T. T. Wu and C. N. Yang, Phys. Rev. D **14**, 437 (1976).
[19]C. W. Misner, K. S. Thorne, and J. A. Wheeler, *Gravitation* (Freeman, San Francisco, 1973), Chap. 4.
[20]See Ref. 5, p. 15.
[21]Reference 5, p. 136.
[22]R. Abraham and J. E. Marsden, *Foundations of Mechnics* (Benjamin, Reading, MA, 1978), 2nd ed., p. 154.
[23]F. W. Warner, *Foundations of Differentiable Manifolds and Lie Groups* (Springer, New York, 1983), Chap. 6. The proof of the Hodge decomposition theorem here is for elliptic operators, whereas the wave operator in electromagnetism is hyperbolic.
[24]C. B. Morrey, Jr., *Multiple Integrals in the Calculus of Variations* (Springer, New York, 1966), pp. 295–305.

Cooling by immersion in liquid nitrogen

Thomas W. Listerman, Thomas A. Boshinski, and Lynn F. Knese
Wright State University, Dayton, Ohio 45435

(Received 7 December 1984; accepted for publication 13 May 1985)

When an object is cooled by immersion in a liquid, there is an unexpected increase in the violence of boiling just before the boiling stops. Most people seem fascinated by this phenomenon yet few are acquainted with its explanation in terms of a change in the heat-transfer mechanism from film boiling to nucleate boiling. We have developed two variations of an intermediate level undergraduate laboratory experiment to measure the heat-transfer rate after a sample is immersed in liquid nitrogen. The temperature of the sample, as measured by a thermocouple, is recorded as a function of time using either a potentiometer strip-chart recorder or a digital voltmeter–microcomputer combination. The heat-transfer rate as a function of sample temperature is computed from these results, and the reason for the effect is clearly seen.

I. INTRODUCTION

When a metal object such as a steel bolt is suddenly immersed in liquid nitrogen, the liquid starts boiling violently. As time goes on, the violence of the boiling slowly decreases, and soon it appears as if the boiling is just about to stop. But instead of stopping, there is suddenly a big increase in the violence of boiling and then the boiling stops.

If you have never seen this effect for yourself, you may question whether it really occurs. You can easily observe it if liquid nitrogen is available and may already have observed it when filling a room temperature vacuum system cold trap with liquid nitrogen. If liquid nitrogen is not available, you can see the same effect by dropping an incandescent piece of metal into water.

The explanation for this effect, called the Leidenfrost effect,[1] lies in the nature of heat transfer between a solid surface and a colder surrounding liquid.[2] This apparently simple process consists of six distinct and identifiable regimes of pool boiling.

Figure 1 shows the principal boiling regimes of water at atmospheric pressure as reported by Farber and Scorah.[3] In their experiment, an electrically heated platinum wire was immersed in water, and the power input Q required to maintain the wire at various temperatures T above the saturation temperature of the water T_{SAT} was measured.

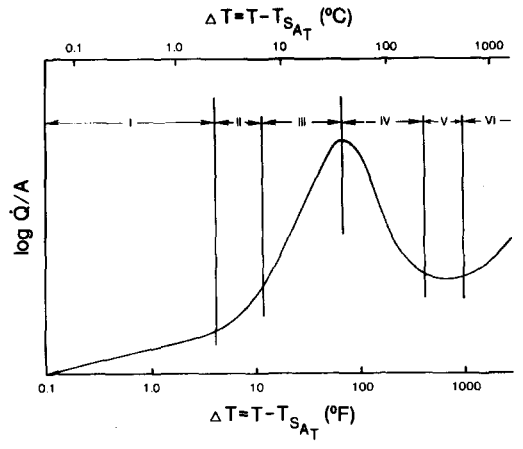

Fig. 1. $\dot{Q}/A$ versus temperature difference between platinum wire and water bath.

(The saturation temperature of a liquid is the normal boiling temperature of the liquid at the existing pressure.) The logarithm of the power input per unit area of the platinum wire $\dot{Q}/A$ was then plotted against the logarithm of the difference between the temperature of the wire and the saturation temperature of the liquid $(T - T_{SAT})$. $\dot{Q}$ was divided by A in an attempt to scale the heat-transfer rate data so the results displayed in Fig. 1 could be applied to any object immersed in water.

The first regime of boiling is characterized by free-convection. The superheated liquid next to the warm solid surface is convected to the liquid–air surface where the energy is released by evaporation. Convection is dominant only when the solid is no more than a few degrees warmer than the liquid and does not transfer heat very efficiently, since both the heat capacity of the liquid and the buoyant forces driving the convection current are small.

At higher temperatures nucleate boiling occurs. In the second regime bubbles form at so-called nucleation sites on the solid surface and detach. As the bubbles rise, they are reabsorbed by the liquid, and the energy reaches the liquid–air interface by convection. Once the bubbles reach the liquid–air interface and directly release their vapor, the boiling is said to be in the third regime. Nucleate boiling is a more efficient heat transfer mechanism than convection because the latent heat of vaporization is much larger than the product of the heat capacity and the small temperature increase of the water encountered in convection.

Once the violence of nucleate boiling reaches a critical value, the bubbles begin to coalesce before they detach and form a thin unstable vapor film around parts of the solid. The heat-transfer rate in this fourth regime is lower than that for nucleate boiling because energy must be conducted through the thin vapor film to its outer edges where bubbles form.

A stable vapor film envelopes the sample at higher temperatures, and in this fifth regime the heat-transfer rate remains roughly constant. At even higher temperatures, energy transfer through the vapor film due to radiation becomes significant, and the heat-transfer rate rises in this sixth regime.

Cooling by immersion may be explained straightforwardly in terms of these regimes of boiling. When a room-temperature object is first immersed in liquid nitrogen, it is surrounded by a vapor film. As the object slowly cools through the sixth and fifth boiling regimes, the violence of boiling decreases with the heat transfer rate. Finally, the vapor film becomes unstable and collapses, and the sample rapidly cools through the fourth, third, and second regimes as the heat-transfer rate increases by more than an order of magnitude. This corresponds to the sudden increase observed in the violence of bubbling. The boiling then enters the first regime in which all heat transfer is by convection, and no bubbles are observed.

II. EXPERIMENT

We have developed two variations of an intermediate level laboratory experiment to measure the heat-transfer rate as a function of temperature for objects immersed in liquid nitrogen. In each version of the experiment, the temperature of a copper cylinder was measured as a function of the time after immersion. The cylinder we used was 5.08 cm in diameter, 7.25 cm long, and had a mass of 1.34 kg. A sample this massive was chosen to lengthen the cool-down time and make semiautomated data taking easier. A high thermal conductivity copper sample was chosen so we could assume that the temperature is essentially the same at all points in the sample as it cools.[4] Sample temperatures were measured with a chromel–alumel thermocouple which had one junction soldered into a small hole in the surface of the sample. The reference junction of the thermocouple was immersed in an ice bath. The two experimental versions of the experiment differ in how thermocouple emfs were measured as a function of time.

The first variation was similar to the experiment of Merte and Clark.[5] The thermocouple leads were connected to a potentiometer, and the imbalance of the potentiometer was recorded on a strip-chart recorder. Merte and Clark set the potentiometer and recorder so the entire cooldown was recorded across the width of the strip chart without any changes in dial settings. Voltage imbalance and time readings were then determined directly from the strip chart for their analysis. We chose a much larger sample to lengthen the cool-down time and eliminate the need to take voltage imbalance measurements from the strip chart. As our sample cooled, the time when the potentiometer was balanced for a particular potentiometer dial setting was indicated by the location of the null crossover on the strip chart. This, of course, indicated the time the sample temperature reached the value corresponding to the emf set on the potentiometer dials. The potentiometer dial setting was written on the strip chart next to the corresponding null crossover, the dail setting was changed, and the entire procedure was repeated over and over to follow the sample temperature during cooling. The resulting table of thermoelectric emf values as a function of time after immersion was analyzed to determine the heat-transfer rate as a function of sample temperature.

The second variation of the experiment replaced the potentiometer and strip-chart recorder with a digital voltmeter read at a predetermined rate by a computer. This rate was increased during the experiment since cooling was very rapid once the vapor layer collapsed. Figure 2 shows a sample set of thermoelectric emf versus time-after-immersion data obtined by this second variation of the experiment.

We began the analysis of the data with the conversion of the emf versus time data to temperature versus time data

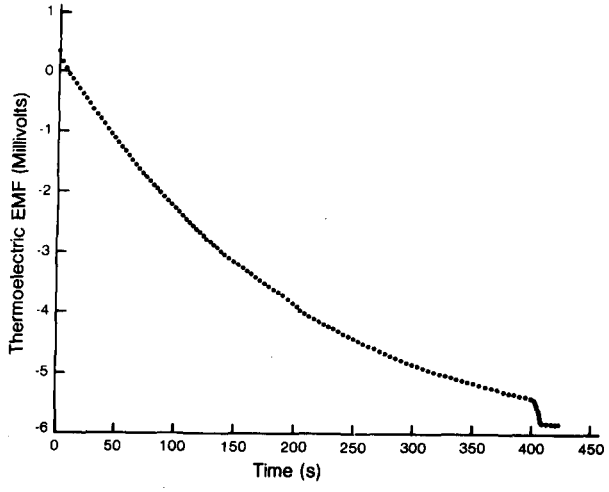

Fig. 2. Thermoelectric emf versus time after immersion.

using standard thermocouple calibration tables.[6] At first, this conversion, along with the rest of the analysis, was done by hand. Later, when the second version of the experiment resulted in large numbers of data points per run, the entire analysis was carried out on a computer. (It is still useful, however, for students to analyze a few data points by hand to learn the analysis procedures.) The hand procedures can be automated straightforwardly. Data from the standard thermocouple tables must first be entered into a computer file. Temperatures can then be determined by having the computer search for measured emfs in the table and interpolate between tabular values. We chose instead to represent the data in the calibration tables by a power series in thermoelectric emfs and to directly compute temperatures using this series representation. Both the least-square fitting to the power series and the temperature computation were performed with extended precision FORTRAN programs to ensure the same accuracy previously obtained with hand conversion. Figure 3 shows the same data as in Fig. 2 converted to sample temperature versus time-after-immersion data by this procedure.

Since we have assumed the temperature is the same throughout the volume of the sample, the rate of heat loss per unit sample surface area is given by

$$\frac{\dot{Q}}{A} = \left(\frac{n}{A}\right) C_p(T) \frac{dT}{dt}.$$

In this equation, A is the surface area, n is the number of moles, $C_p(T)$ is the molar heat capacity at constant pressure at the temperature T, and dT/dt is the slope of the temperature–time curve. We determined the slope of this curve at a particular point by assuming adjacent data points could be connected by a straight line and determining its slope. When we first planned this experiment, we assumed that a more complicated procedure, including data smoothing to remove random error in the data points, would be required to find this slope. The procedure required that we know the slope of the temperature–emf calibration curve as a function of temperature. This was the reason for the previously mentioned least-square fit of the thermocouple calibration curve to a power series. Fortunately, the simple straight-line procedure for finding the slope yielded results with acceptable random scatter, so the more complicated procedure was never used.

$C_p(T)$ is related to the specific heat at constant volume $C_v(T)$ by the relationship[7]

$$C_p(T) = C_v(T) + VT\beta^2/\kappa,$$

where V is the sample volume, β is the isobaric thermal expansion coefficient, and κ is the isothermal compressibility. The difference between C_p and C_v is $\leqslant 3\%$ for the sample and temperature range used in the experiment[8,9] and was neglected in our analysis.

We can compute C_v using microscopic models undergraduate students have encountered in solid-state physics, modern physics, and statistical thermodynamics courses. For our copper sample it may be written as the sum of an electronic contribution γT and a lattice (phonon) contribution $C_l(T)$[9]:

$$C_v(T) = \gamma T + C_l(T).$$

In the temperature range encountered, the γT term was always $< 1\%$ of $C_l(T)$[9] and was neglected in our analysis. (Students can be asked to justify both this assumption and that of the equality of C_p and C_v in their reports.) Since the lattice contribution varies strongly with temperature, we should compute it using the Debye model[10] including the temperature variation of the Debye characteristic temperature θ_D.[11] Since for copper $\theta_D(T)$ monotonically increases from 315–321 K as the temperature rises from 77–300 K,[11] this variation was ignored and a constant $\theta_D = 315$ K used. This leads to a maximum error in C_v of $\sim 0.1\%$ at $T = 300$ K.[9] The Debye model itself is difficult to use in the analysis since it yields an expression for C_v containing an integral with θ_D/T as the upper limit. (The simple one- or two-term power series approximation applies only at temperatures much lower than those encountered in this experiment.) Tabulated results of a numerical integration of this expression are available[12] for hand analysis of data. A series solution to the expression is also available[13] which could be used to evaluate C_l.

The Einstein model,[14] on the other hand, yields a simple,

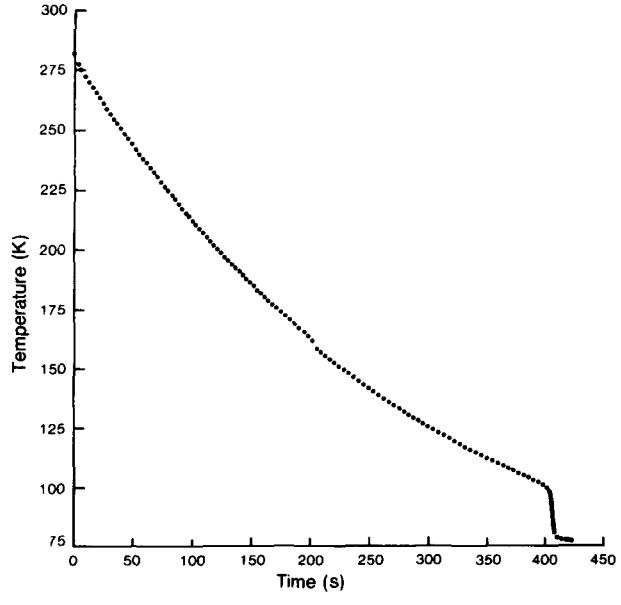

Fig. 3. Sample temperature versus time after immersion.

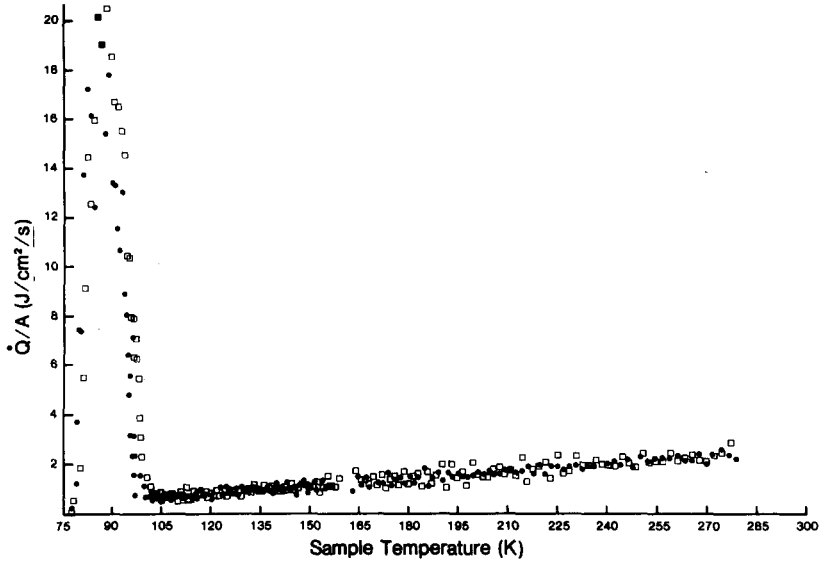

Fig. 4. $\dot{Q}/A$ versus sample temperature.

although less accurate, expression for the lattice heat capacity:

$$C_l = 3R\left(\frac{\theta_E}{T}\right)^2 \frac{\exp \theta_D/T}{[\exp(\theta_D/T) - 1]^2}.$$

In this expression, R is the gas constant and θ_E is the Einstein characteristic temperature of the solid. Due to the similarity of the predictions of the two models at all except the lowest temperatures,[15] we found the Einstein model gave a reasonable approximation to the Debye model when we let $\theta_E = 0.77\ \theta_D$. This procedure yielded C_v values which differed from those of the Debye model by about 5% at 77 K. At higher temperatures this difference decreased to less than 0.02% at 300 K. A more accurate approximation of this sort is that of Listerman and Ross[16] in which a temperature-dependent θ_E is given by

$$\theta_E/T = \theta_D\,[a + b \exp(-cT/\theta_D)],$$

where

$$a = 0.768\,712\,526\,726\,1697,$$
$$b = 0.264\,790\,644\,105\,7428,$$
$$c = 9.168\,685\,063\,692\,587$$

is used. In the temperature range of $0.2 \leqslant T/\theta_D \leqslant 12$ the average difference between this approximation and the Debye model was 0.036%. The approximation of Listerman and Ross was used in analyzing the results reported here.

The results of this analysis for two different experimental runs are shown in Figs. 4 and 5. Figure 4 shows $\dot{Q}/A$ versus sample temperature. The big increase in the heat-transfer rate just before the sample reaches liquid nitrogen temperature is clearly seen in this figure. The logarithm of $\dot{Q}/A$ versus the logarithm of the difference between the sample and saturation temperatures is shown in Fig. 5. This result is of the same form as the data for water shown in Fig. 1 and is in agreement with the data of Merte and Clark for liquid nitrogen.

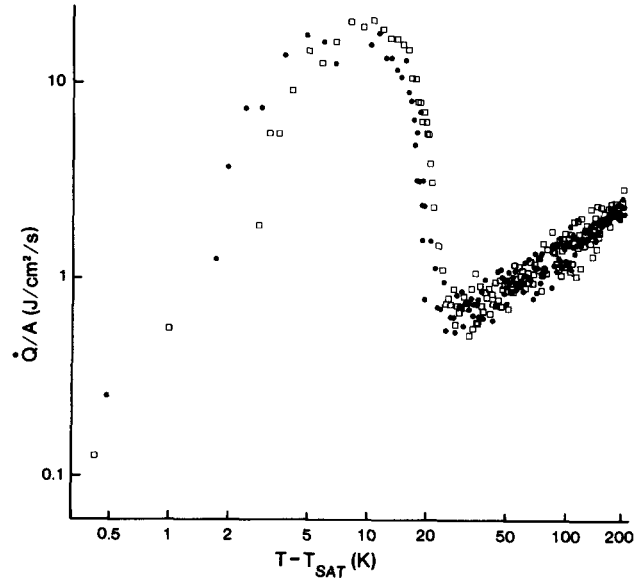

Fig. 5. $\dot{Q}/A$ versus temperature difference between sample and liquid nitrogen bath.

III. CONCLUSIONS

We found this to be a useful intermediate laboratory experiment for several reasons. It exposed students to interesting heat-transfer phenomena not typically mentioned in physics courses. Students learned experimental skills related to the handling and use of cryogenic fluids, to thermoelectric thermometry, and to automated data taking. The Einstein and/or Debye models studied in class were used in analyzing data along with other results related to heat capacity. Additionally students may gain a good deal of experience in programming and computer analysis of data.

The experiment can also evolve over time as succeeding groups of students make modifications and improvements. The experiment itself can evolve from the first to the second variation. The analysis could evolve from using the simple Einstein model to using the temperature-dependent θ_E Einstein model to using the actual Debye model formulas. Corrections can be included for the electronic contribution to the specific heat, for the temperature dependence of θ_D, and for the difference between C_p and C_v. The random error in the results may be significantly reduced by

improving the procedure for determining the slope of the temperature–time curve. Rather than using only two data points, several points centered about the temperature of interest can be least-square fitted to a three-term power series. The least-square fitting removes much of the random error in the data points and the slope at the temperature of interest may be computed from the fitted curve.

In addition, the variation of the heat-transfer rate with changes in the details of the experiment may be studied. Dividing the heat-transfer rate by the sample surface area is a simple attempt to scale the results so that they can be applied to any solid transferring heat to the liquid. By using different metal samples, different surface textures, different shapes and sizes, and different sample orientations a wide range of original experiments may be performed.

[1]F. L. Curzon, Am. J. Phys. **46**, 825 (1978).

[2]J. Walker, Sci. Am. **247**, 162 (December, 1982).

[3]E. H. Farber and R. L. Scorah, Trans. ASME **70**, 369 (1948).

[4]The cooling of solids subject to abrupt changes of surface temperature was studied by E. D. Williamson and L. H. Adams, Phys. Rev. **14**, 99 (1919) and their results are summarized by E. U. Condon, in *Handbook of Physics*, edited by E. U. Condon and H. Odishaw (McGraw–Hill, New York, 1967), 2nd ed., pp. 5–64,5. Their results show that if the surface of a copper cylinder 5.08 cm in both diameter and length is abruptly cooled by 7 °C when $T\sim 80$ K, the temperature in the center of the copper cylinder should be only ~ 0.8 °C higher than the surface temperature after 1 s. Our highest cooling rate was 7 °C/s at ~ 90 K and their result suggests that the temperature in the center of our sample may lag behind the surface temperature by about 1 °C.

[5]H. Merte and J. A. Clark, Adv. Cryogenic Eng. **7**, 546 (1962).

[6]*The Omega Temperature Measuring Handbook* (Omega Engineering, Stamford, CT, 1974), p. A9.

[7]M. W. Zemansky and R. H. Dittman, *Heat and Thermodynamics* (McGraw–Hill, New York, 1981), 6th ed., p. 228.

[8]E. S. R. Gopal, *Specific Heats at Low Temperatures* (Plenum, New York, 1966), p. 9.

[9]M. W. Zemansky and R. H. Dittman, Ref. 7, pp. 314–322.

[10]M. W. Zemansky and R. H. Dittman, Ref. 7, pp. 308–311.

[11]D. L. Martin, Can. J. Phys. **38**, 17 (1960).

[12]E. S. R. Gopal, Ref. 8, pp. 221–226.

[13]*Landolt–Bornstein Zahlenwerte and Functioner der Physik, Chemie, Astronomie, Geophysik, und Technik* (Springer, Berlin, 1961), Vol. II, Part IV, p. 742.

[14]M. W. Zemansky and R. H. Dittman, Ref. 7, pp. 303–309.

[15]E. S. R. Gopal, Ref. 8, p. 27.

[16]T. W. Listerman and C. Ross, Cryogenics **19**, 547 (1979).

Classical dynamics and Lie groups

J. D. Louck and N. Metropolis

Theoretical Division, Los Alamos National Laboratory, Los Alamos, New Mexico 87545

(Received 12 February 1985; accepted for publication 21 April 1985)

The phase space time evolution operator for a dynamical system is derived directly from Newton's equation of motion. This operator is used to show, in an elementary way, how a Lie group enters into the description in phase space of the path of a one-dimensional damped, driven, harmonic oscillator. Concepts from Lie group theory are thus illustrated in a nontrivial but elementary and familiar setting. Generalizations of this method for Hamiltonian systems are outlined in a series of remarks that suggest the broader scope of the subject.

I. INTRODUCTION

The time evolution of physical quantities in classical dynamics can be presented in a form that is closely related to the time evolution of the corresponding quantity in quantum dynamics. The purpose of this paper is to present this operator formulation of classical mechanics and to illustrate its application to several elementary and familiar dynamical systems.

Consider Newton's equation of motion in one dimension,

$$a_t = f_t(x_t, v_t), \tag{1}$$

where $f_t(x_t, v_t)$ denotes the force per unit mass, x_t the position at time t of a point particle of mass m relative to an inertial reference frame, $v_t = \dot{x}_t$ the directed speed at time t, and $a_t = \ddot{x}_t$ the acceleration at time t. The force function $f_t(x_t, v_t)$ is assumed to be a smooth function of x_t, v_t, and t (continuous derivatives of all orders with respect to these variables). If the solution x_t to Eq. (1) is analytic at all times t, then the solution is given by

$$x_{t+\tau} = e^{t\Omega_\tau} x_\tau, \tag{2a}$$

where x_τ is the position of the particle at time $\tau \leqslant t$ and Ω_τ is the differential operator defined by

$$\Omega_\tau = v_\tau \left(\frac{\partial}{\partial x_\tau}\right) + f_\tau(x_\tau, v_\tau)\left(\frac{\partial}{\partial v_\tau}\right) + \left(\frac{\partial}{\partial \tau}\right). \tag{2b}$$

This result is easily proved by repeatedly differentiating Eq. (1) with respect to t and substituting the k th such derivative into the Taylor series expansion

$$x_{t+\tau} = \sum_{k=0}^{\infty} \left(\frac{t^k}{k!}\right)\left(\frac{d^k x_t}{dt^k}\right)_{t=\tau}. \tag{3}$$

The operator $\exp(t\Omega_\tau)$ is itself defined by

$$\exp(t\Omega_\tau) = \sum_{k=0}^{\infty} \left(\frac{t^k}{k!}\right)\Omega_\tau^k. \tag{4}$$